Materials Physics and Mechanics 29 (2016) 76-81 Received: October 26, 2016

THE STRUCTURAL PROPERTIES OF ELASTICALLY STRAINED InGaAlAs/InGaAs/InP HETEROSTRUCTURES GROWN BY MOLECULAR BEAM EPITAXY

I.I. Novikov[1,2*], A.V. Babichev[1,2], E.S. Kolodeznyi[2], A.S. Kurochkin[1,2], A.G. Gladyshev[1,2], L.Ya. Karachinsky[1,2], V.N. Nevedomsky[3], S.A. Blokhin[3], A.A. Blokhin[3], A.M. Nadtochiy[3], A.Yu. Egorov[1,2]

[1]Connector Optics LLC, Domostroitelnaya 16, Saint Petersburg, 194292, Russia.

[2]ITMO University, Kronverkskiy 49, Saint Petersburg, 197101, Russia.

[3]Ioffe Institute, Polytechnicheskaya 26, Saint Petersburg, 194021, Russia.

*e-mail: Innokenty.Novikov@connector-optics.com

Abstract. The paper discussed the results of the study of elastically strained InGaAlAs/InGaAs/InP heterostructures grown by molecular beam epitaxy as active region for laser diodes of the spectral range 1510-1580 nm. Structural and optical properties of the heterostructures were studied by transmission electron microscopy and photoluminescence techniques. We obtained the dependence of the critical thickness of multiple elastically strained InGaAs layers separated by InGaAlAs barriers on mole fraction of InAs.

1. Introduction

Rapid growth of information capacity raises new challenges and new demands for optical networks and specifies new requirements for transmission units [1]. The most important ones are increasing of transmission speed and energy performance. An additional point is that the energy spent on data transfer is grown too and, as a consequence, there appears a need in energy efficient laser emitters capable to operate at low pump currents. Vertical-cavity surface-emitting laser (VCSEL) provides the most energy efficient data transfer [2]. The main advantages of VCSEL over the edge-emitting laser are low threshold current and ability to operate without cooling at high data transfer rate [2]. By now, the direct modulation frequency of 20 GHz has been achieved for VCSEL of the 1520-1580 nm spectral range [3, 4]. Further increasing of the modulation frequency could be associated with increase of the differential gain in active region of the laser diode that can be achieved by increasing of the mechanical stress in quantum wells (QWs) [4, 5]. Having used triple and fourfold solid solutions InGaAs and InAlGaAs it is possible to fabricate elastically strained QWs with mismatch parameter (MP) about 1-2 % between crystal lattice of the QW and the substrate [6]. Along with increasing of the differential gain, the elastically strained QWs can get smaller thicknesses i.e. 2-4 nm. As a result, with the total heterostructure thickness of 80-90 nm it is possible to fabricate a larger number of QWs and made a VCSEL with superior optical amplification at 1550 nm near the maximum intensity of the optical mode in the cavity. Therefore, it is important to experimentally determine the maximum number of QWs with a maximum possible MP between lattice parameter of the QWs and the substrate for fabrication of the VCSEL active region with high radiation efficiency and good reliability. In

this paper, we reported on studies of structural and optical properties by transmission electron microscopy (TEM) and photoluminescence (PL) spectroscopy of the elastically strained InGaAs QWs that allows to define the critical thickness of elastically strained InGaAs layers grown on InP substrate depending on InAs mole fraction.

2. Experiment

Experimental samples (ES) of elastically strained heterostructures InGaAlAs/InGaAs/InP were grown by molecular beam epitaxy (MBE) on InP substrate (100) [7]. The fabricated heterostructures were consisted of 5 QWs forming from narrow-bandgap $In_xGa_{1-x}As$ layers ($0.67 \leq x \leq 0.82$) and wide-bandgap barriers $In_{0.53}Al_{0.20}Ga_{0.27}As$ with thickness 10 nm. In order to have a constant maximum of the PL spectrum near wavelength of 1520±10 nm we changed the composition, thicknesses of $In_xGa_{1-x}As$ layers and MP between $In_xGa_{1-x}As$ and InP substrate correspondingly. We fabricated ES with the following MPs: 1.0, 1.3, 1.6 and 2 %. Chemical composition, thickness, MP, position of the maximum of the PL spectrum and full width of the PL spectrum at half maximum (FWHM) for the all ES are shown in Table 1.

Table 1. Characteristics of fabricated ES.

№	Material of QW	Number of QWs	Barrier/QW thickness, nm	MP, %	Maximum of the PL spectrum, nm	FWHM, meV
C1	$In_{0.67}Ga_{0.33}As$	5	10.0/3.2	+1.0	1519	25
C2	$In_{0.72}Ga_{0.28}As$	5	10.0/2.7	+1.3	1521	31
C3	$In_{0.76}Ga_{0.24}As$	5	10.0/2.5	+1.6	1524	43
C4	$In_{0.82}Ga_{0.18}As$	5	10.0/1.9	+2.0	1526	345

PL spectra were measured at the liquid nitrogen and room temperatures using an experimental setup including monochromator, pumping laser with wavelength of 532 nm (double frequency of YAG:Nd), cooled Ge photodiode and lock-in amplifier. The optical power of the exciting laser was attenuated by optical filters. Visual inspection of the integrity of epitaxial layers was controlled by TEM method. Samples for TEM were prepared in cross section geometry by a conventional method of pre-thinning by mechanical grinding, polishing and finishing surface cleaning by argon ions with energy of 4 keV at the glancing angle to the surface. We used the optical imaging regimes with diffraction contrast in two-beam conditions during the study of the ESs by TEM method.

3. Experimental results and discussion.

PL spectra of the ESs C1, C2 and C3 at the room and liquid nitrogen temperatures for two different power densities of the exciting laser are shown in Fig. 1. One could observe that the PL spectra of the ESs C1 and C2 had the typical for QW shape with a single peak described by a Lorentz function. FWHM for low pump density (density pump – 50 W/cm^2) and 77 K was 20 and 27 meV for the C1 and C2 structures, respectively, what indicated on a good uniformity of the QW composition and thickness. However, PL spectrum of the ES C3 measured at room temperature for low pumping density contained additional long-wave peak (marks with an arrow) corresponding to the emission from regions with a higher content of In. At 77 K and low pumping density the long-wave peak was dominant and saturated with increase of pumping power, but at high pumping density (690 W/cm^2) main short-wave peak was dominant. The behavior of the PL spectra indicated on strong heterogeneity of the

chemical composition of the QWs in the ES C3. Due to the fact that the long-wave peak was saturated with increase of laser pumping power it was assumed that the heterogeneity may not be presented in all QW, but only in one or two. Most likely, during the MBE growth of the C3 structure thickness of $In_{0.76}Ga_{0.24}As$ QW layer exceeded the critical value and, as a result, regions with various content of In were formed due to the self-organization of three-dimensional islands from the QW material. To check the assumptions, we conducted study of heterostructures by the TEM.

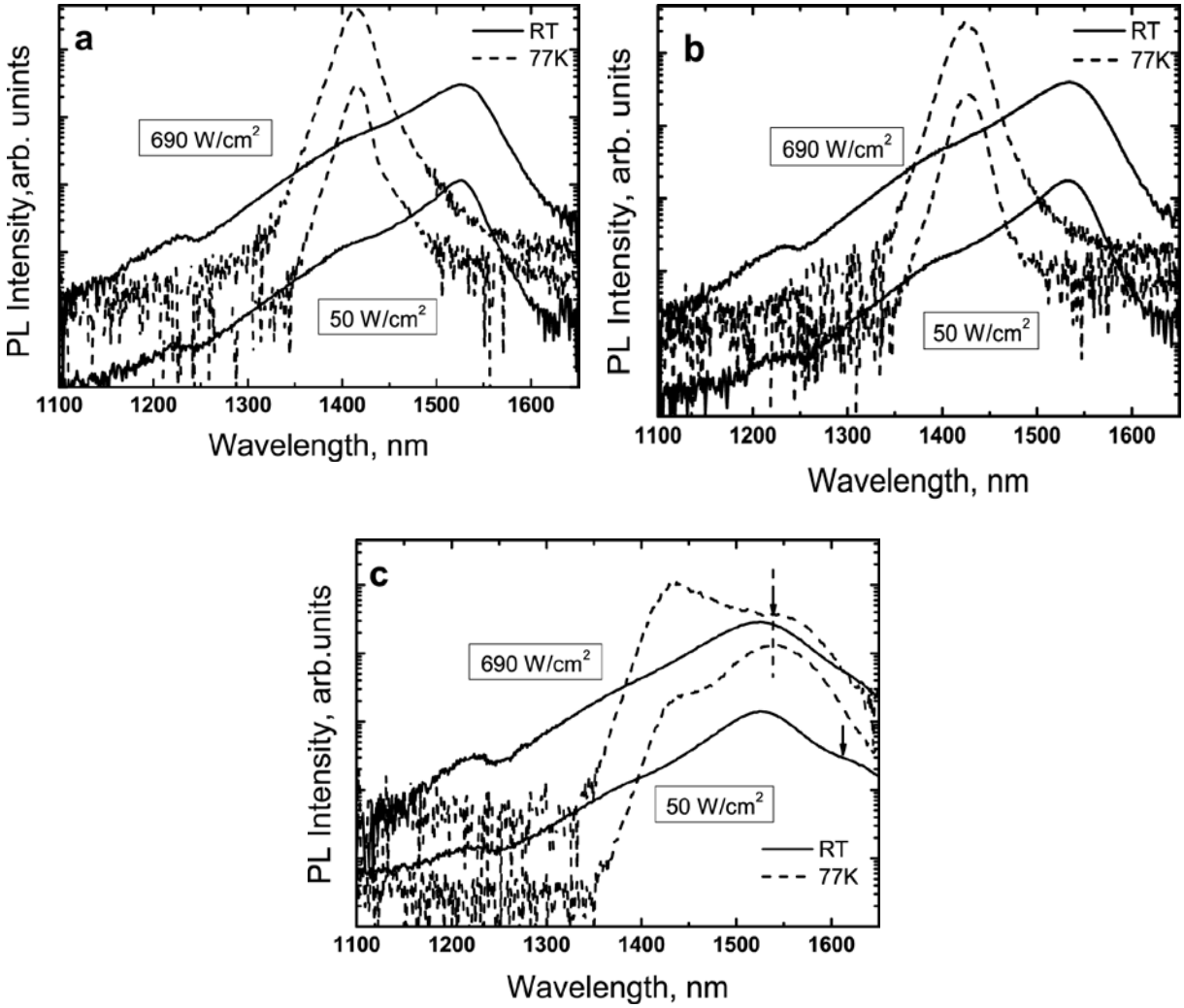

Fig. 1. PL spectra of ESs C1(a), C2 (b) и C3 (c) at the room and liquid nitrogen temperatures for two different power densities of the exciting laser.

Figure 2 shows TEM image of cross section of ESs C1-C4 in reflection sensitive to chemical composition. Investigated samples had planar interfaces.

However, in reflection sensitive to the stress (Fig. 3) it is impressive to see that the areas of the stress concentration leading to the occurrence of structural defects were appeared with increasing of MP up to 1.6 % (ES C3).

The image contrast reflected the change in the chemical composition of the samples. It is seen that QWs of the ES C3 in some places had a non-uniform thickness. Thus, resulting islands formed the interconnected area. Examination of samples showed that in the ESs C1-C2 were dislocation density was less than 1×10^6 cm^{-2} (below the detection). However, in the ESs C3 and C4 dislocation pile-ups were appeared above the active region (Fig. 4, C4). The dislocation density in the pile-ups was approximately 1×10^{10} cm^{-2}.

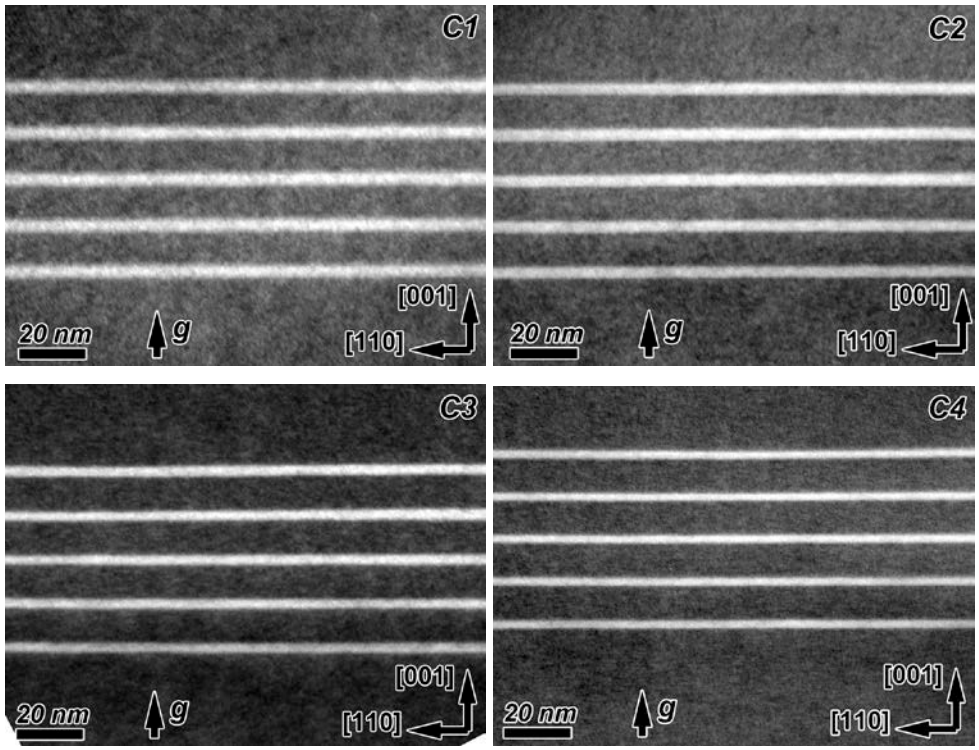

Fig. 2. TEM image of cross section (1-10) of ESs C1-C4 obtained in two-beam conditions with g-vector =[002]. The contrast of the images demonstrates the change in the chemical composition of the layers.

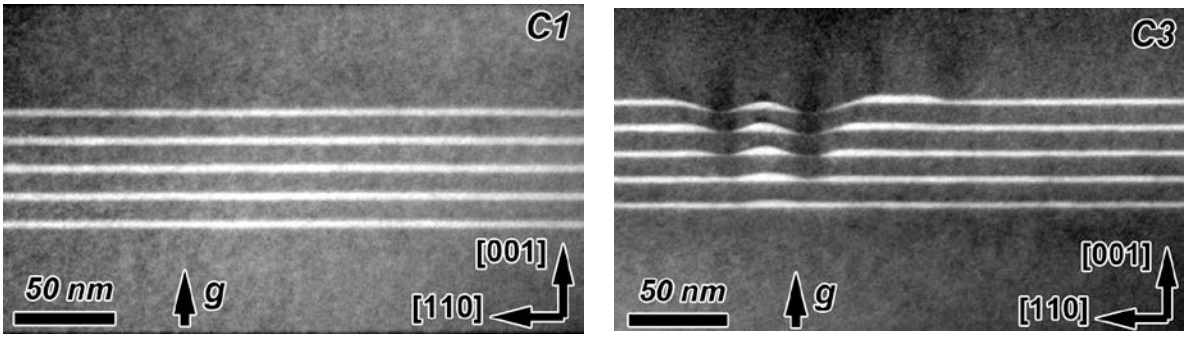

Fig. 3. TEM images of cross section (1-10) for ES C1 (left) and ES C3 (right) obtained in two-beam diffraction conditions with g-vector = [002].

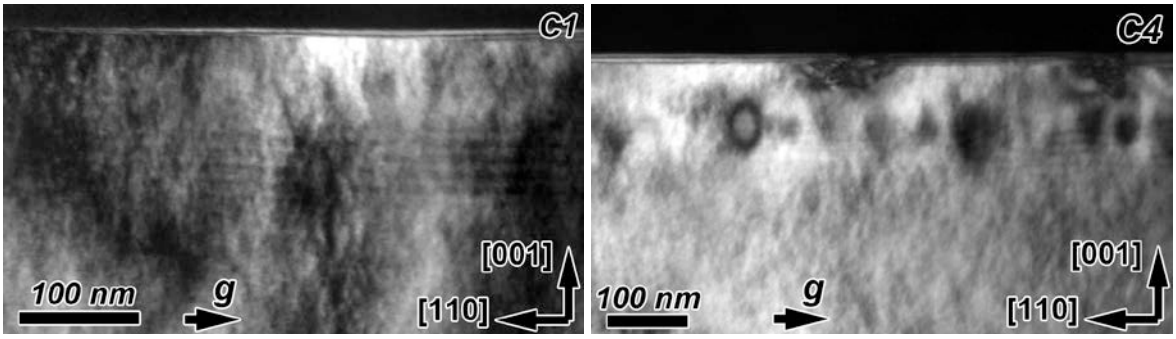

Fig. 4. TEM image of cross section (1-10) for the ES C1 (left) and ES C4 (right) obtained in two-beam diffraction conditions with g-vector [-2-20]. Changing the contrast of images reflects the change of elastic stresses in the samples.

The analysis of the PL spectra of the ESs allowed to determine the critical thickness of the QWs with different In content using Matthews–Blakeslee theory (the case of an anisotropic modulus of elasticity and inequality of the shear modulus of the substrate and the epitaxial layer) [8]. The theoretical dependence of the critical thickness of InGaAs layer on InP substrate on mole fraction of InAs is shown in Figure 5. Analyzing the measurements of the PL spectra, we divided ESs into two allocated groups: first one with active region thickness less than the critical value and second one where the thickness of active region is greater than the critical value and formation of islands with high In content was occurred. The criterion was the appearance of an additional long-wave shoulder in the PL spectrum at room temperature [7], as well as features identified by TEM. The average values of In mole fraction and the total thickness of the active region are shown in Table 2. The results indicated that ESs C1 and C2 had thicknesses of the active region less than the critical value samples. On Fig. 5 the experimental points corresponding to mentioned ESs lie down below or near theoretical curve. The ESs C3 and C4 had thicknesses of the active region greater than the critical value and the corresponding experimental points lie above the theoretical curve. Comparing the experimental data, we made a conclusion that the real critical thickness of the InGaAs layer is close to calculated theoretical value. Experimental curve shown in Figure 5 by a dotted line and based on the results of current study was higher than the theoretical curve. The difference between the critical thickness of the theoretical and experimental curves for InGaAs layer was about 6-7 nm.

Table 2. InAs molar fraction and the total thickness of the ES active region.

ES number	Active region	The averaged values of the molar fraction	Total thickness, nm
C1	$(In_{0.67}Ga_{0.33}As)\times5+(In_{0.53}Al_{0.20}Ga_{0.27}As)\times4$	0.570	56.0
C2	$(In_{0.72}Ga_{0.28}As)\times5+(In_{0.53}Al_{0.20}Ga_{0.27}As)\times4$	0.578	53.5
C3	$(In_{0.76}Ga_{0.24}As)\times5+(In_{0.53}Al_{0.20}Ga_{0.27}As)\times4$	0.585	52.5
C4	$(In_{0.82}Ga_{0.18}As)\times5+(In_{0.53}Al_{0.20}Ga_{0.27}As)\times4$	0.586	49.5

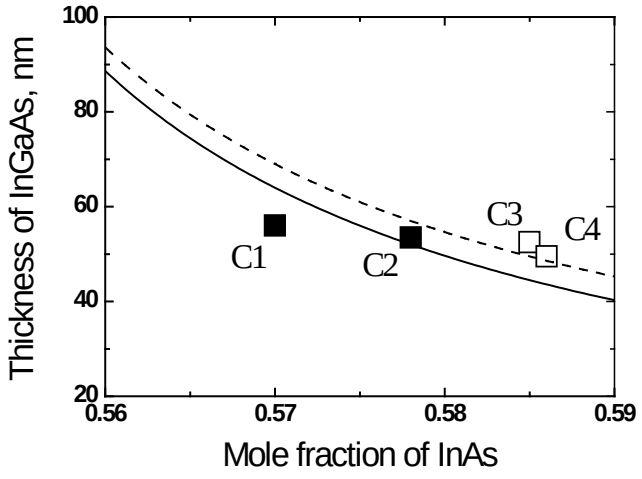

Fig. 5. Dependence of critical thickness of InGaAs layers grown on InP substrate on mole fraction of InAs: solid line - theoretical dependence [8];
dashed line - experimental dependence;
■ - ES with active region where thickness is less critical thickness;
□ – ES with active region where thickness is greater than the critical thickness

4. Conclusions

The elastically strained heterostructures with InGaAs QWs with different composition emitting in the spectral range of 1520 ± 10 nm were grown on InP substrates by MBE technique. The lattice mismatch of QWs material and InP substrate was 1.0, 1.3, 1.6 and 2.0 %. The TEM and PL results had shown the spontaneous formation of regions with high In content in heterostructures with lattice mismatch values of 1.6 and 2.0 % that lead to degradation of their optical properties. As a result, the dependence of critical thickness of InGaAs layers grown on InP substrate on InAs mole fraction was obtained. The analysis of the critical thickness in heterostructures with InGaAs QWs showed that the experimental value of the critical thickness was close to the theoretical curve. The difference between the critical thickness was about 6-7 nm. It was found that the total thickness of InGaAs QWs with lattice mismatch values of 1.6 and 2.0 % is higher than the critical value. The experimental results can be used in the development of laser heterostructures based on elastically strained InGaAs QWs.

Acknowledgment

This work was supported by the Ministry of Education and Science of the Russian Federation in the framework of the Federal Target Program "Research and development on priority directions of scientific-technological complex of Russia for 2014-2020", the code 2015-14-579-0014, agreement № 14.579.21.0096, unique ID RFMEFI57915X0096.

References

[1] N.K. Vlachos // *American Journal of Advanced Computing* **2(3)** (2015) 71.

[2] P. Moser, J.A. Lott, P. Wolf, G. Larisch, A. Payusov, N.N. Ledentsov, W. Hofmann, D. Bimberg // *IEEE Photonics Technology Letters* **24(1)** (2012) 19.

[3] D. Ellafi, V. Iakovlev, A. Sirbu, G. Suruceanu, Z. Mickovic, A. Caliman, A. Mereuta, E. Kapon // *Optics Express* **22(26)** (2014) 32180.

[4] S. Spiga, D. Schoke, A. Andrejew, M. Müller, G. Boehm, M.C. Amann, In: *Optical Fiber Communication Conference* (Optical Society of America, Anaheim, CA, USA, 20–22 March 2016), p. Tu3D-4.

[5] D. Nichols, P. Bhattacharya // *Applied Physics Letters* **61(18)** (1992) 2129.

[6] A.V. Babichev, A.S. Kurochkin, E.S. Kolodeznyi, A.G. Gladyshev, I.I. Novikov, L.Y. Karachinsky, A.Y. Egorov // *Materials Physics and Mechanics* **24** (2015) 284.

[7] A.G. Gladyshev, I.I. Novikov, L.Ya. Karachinsky, D.V. Denisov, S.A. Blokhin, A.A. Blokhin, A.M. Nadtochiy, A.S. Kurochkin, A.Yu. Egorov // *Semiconductors* **50** (2016) 1186.

[8] J.W. Matthews, A.E. Blakeslee // *Journal of Crystal Growth* **27** (1974) 118.